Carbohydrate Polymers 80 (2010) 977–983

Contents lists available at ScienceDirect

Carbohydrate Polymers

journal homepage: www.elsevier.com/locate/carbpol

Evaluation of water soluble β-D-glucan from *Auricularia auricular-judae* as potential anti-tumor agent

Zhaocheng Ma [a], Jianguo Wang [a], Lina Zhang [a,*], Yufeng Zhang [b], Kan Ding [c]

[a] *Department of Chemistry, Wuhan University, Wuhan 430072, PR China*
[b] *School of Stomatology, Wuhan University, Wuhan 430079, PR China*
[c] *Glycochemistry & Glycobiology Lab, Shanghai Institute of Materia Medica, Chinese Academy of Sciences, Shanghai 201203, PR China*

ARTICLE INFO

Article history:
Received 20 July 2009
Received in revised form 9 January 2010
Accepted 11 January 2010
Available online 15 January 2010

Keywords:
Auricularia auricula-judae
Polysaccharide
Anti-tumor activity
Apoptosis

ABSTRACT

A water soluble β-D-glucan was isolated by 70% ethanol aqueous solution from *Auricularia auricula-judae,* coded as AAG. AAG exhibited strong inhibition against Acinar cell carcinoma (ACC) proliferation. The *in vivo* tests showed that AAG significantly inhibited tumor growth in a dose-dependent fashion, but not because of cytotoxicity. All the doses showed certain inhibition ratios against tumor-cell growth, while the dose of 20 mg/kg exhibited highest anti-tumor activities. Moreover, the enhancement ratios of body weight for all the doses were significantly higher than that for 5-fluorouracil (5-Fu). Fluorescence microscopy observed the apoptosis tumor cell induced by AGG sample. The results from TUNEL assay further confirmed the apoptosis in Sarcoma 180 solid tumor. Immunohistochemistry for apoptosis-related proteins Bax and Bcl-2 expression tests revealed that AAG induced S-180 tumor cell apoptosis by up-regulation of Bax and down-regulation of Bcl-2 expression. These findings demonstrated that the AAG has biological activities and could be considered as a candidate for possible anti-tumor drugs.

1. Introduction

Cancer is one of the leading causes of death in the world. The main cause is that they damage immune systems in tumor treatment. So, it is necessary to develop novel anti-tumor agents with administrating immunity potential. Polysaccharides have attracted more attention recently in the biochemical and medical fields because of their anti-tumor and immunomodulating properties (Zhang, Cui, Cheung, & Wang, 2007). Numerous bioactive polysaccharides are considered as immunomodulators affecting on proliferation and differentiation of immune cells and cytokines, interleukins and receptors production due to recognition these compounds by the certain receptors located on the leukocytes and other immune cells that lead to enhance the innate and cell-mediate immune responses (Baea, Janga, & Jinb, 2006; Khalikovaa, Zhanaevaa, Korolenkoa, Kaledinb, & Koganc, 2005; Lavia, Friesemb, Gereshc, Hadarb, & Schwartza, 2006; Moradali, Mostafavi, Ghods, & Hedjaroude, 2007).

Some polysaccharides extracted from Chinese herbal medicines have been reported to possess anticancer activities (Chen et al., 2008; Lia et al., 2004). In our lab, various polysaccharides and their derivatives having anticancer activities have been isolated from *Pleurotus tuber regium* (Tao, Zhang, & Cheung, 2006), *Lentinus Edodes* (Zhang, Li, Xu, & Zeng, 2005), *Poria cocos* (Huang, Zhang, Cheung, & Tan, 2006; Wang, Zhang, Li, Hou, & Zeng, 2004), and *Ganoderma tsugae* mycelium (Peng, Zhang, Zeng, & Xu, 2003). *Auricularia auricula-judae*, an ear-like shaped edible fungi, has potential anti-tumor activities (Misaki & Kakuta, 1995; Misaki, Kakuta, Sasaki, Tanaka, & Miyaji, 1981). In our previous work, the structure of a water soluble β-glucan (AAG) isolated from *Auricularia auricula-judae* has been characterized. It was composed of a main chain of (1 → 4)-linked D-glucopyranosyl with branching points at *O*-6 of (1 → 6)-linked D-glucopyranosyl residues. The content of glucuronic acid is about 19% and the distribution of glucuronic acid was not periodic in the polysaccharide (Ma, Wang, & Zhang, 2008). However, its bioactivities have been never reported. Usually, relatively high molecular weight glucans appear to be more effective anti-tumor activity than those of low molecular weight (Mizuno, 1996). But some medical properties of some mushroom polysaccharides like (1 → 3)-α-glucuronoxylomannans, are not strongly dependent on molecular weights. Their hydrolyzed fractions containing glucuronoxylomannans with molecular weights from 53 to 1000 KDa are as effective as those fractions, having higher molecular weights (Gao, Seljelid, Chen, & Jiang, 1996). It was also reported that differences in molecular weight had no obvious influence on the activities of the heteroglycans. Generally, Genetic alterations resulting in the loss of apoptosis or disturbance of apoptosis-signaling pathways are likely to be critical components of carcinogenesis (Schulte-Hermann, Grasl-Kraupp, & Bursch, 1994). Apoptosis, programmed cell

* Corresponding author. Tel.: +86 27 87219274; fax: +86 27 68754067.
E-mail addresses: zhangln@whu.edu.cn, lnzhang@public.wh.hb.cn (L. Zhang).

0144-8617/$ - see front matter © 2010 Elsevier Ltd. All rights reserved.
doi:10.1016/j.carbpol.2010.01.015

death, is modulated by anti-apoptotic and proapoptotic effectors, which involves a large number of proteins. The proapoptotic and anti-apoptotic members of the Bcl-2 family act as a rheostat in regulating programmed cell death and are considered as targets of anticancer therapy (Baea, Janga, Yimb, & Jin, 2005; Baell & Huang, 2002; Goodsell, 2002). The ratio of death antagonists (Bcl-2, Bcl-xL) to agonists (Bax, Bad, Bid) determines whether a cell will respond to an apoptotic stimulus. Down-regulation of the death suppressor Bcl-2 could inhibit tumor growth via promoting programmed cell death (Zhivotovsky, Orrenius, Brustugun, & Doskeland, 1998). It has been proven that Bax promotes apoptosis whereas Bcl-2 suppresses apoptosis (Ranger, Malynn, & Korsmeyer, 2001). Bax resides in an inactive state in the cytosol of many cells. In response to death stimuli, Bax protein undergoes conformational changes that expose membrane-targeting domains, resulting in its translocation to mitochondrial membranes, where Bax inserts and causes release of cytochrome c to activate caspase-3 and other apoptogenic proteins (Guo et al., 2003; Wolter et al., 1997). When Bax predominates, apoptosis is accelerated and the death repressor activity of Bcl-2 is counteracted (Oltvai, Milliman, & Korsmeyer, 1993).

In the present work, we evaluated *in vivo* anti-tumor activities of the polysaccharide AAG against xenograft Sarcoma 180 tumor cells and in vitro inhibition ratio to the proliferation of Acinar cell carcinoma (ACC) tumor cells. Furthermore, the mechanism of the anti-tumor activities of the AAG were investigated by the morphological approaches (fluorescence microscopy with Hoechst stain) and by TdT-mediated dUTP nick end labeling (TUNEL) technique and immunohistochemical method for apoptosis-related proteins Bcl-2 and Bax, attempting to elucidate the mechanism.

2. Materials and methods

2.1. Isolation and fractionation

AAG was isolated from fruit bodies of *Auricularia auricula-judae*, a commercial product cultivated in Fangxian (Hubei, China) according to previously reported method. AAG is water-dissoluble polysaccharides composed of a main chain of β-(1 → 4)-D-glucan with β-(1 → 6)-D-glucose side groups having molecular weight to be 2.88×10^5 (Ma et al., 2008).

2.2. In vitro anti-tumor test

A colorimetric 3-(4,5-dimethylthiazol-2yl)-2,5-diphenyltetrazolium bromide (MTT) method was used for measuring the proliferation for adherent tumor cells. Acinar cell carcinoma (ACC) tumor cells (1×10^5 cells/mL) were grown in Roswell Park Memorial Institute (EPMI) 1640 medium supplemented with 10% fetal bovine serum (FBS) under atmosphere of 5% carbon dioxide at 37 °C for 72 h, in present of sample at concentrations of 0.005 and 0.05 mg/L in 0.9% aqueous NaCl. The number of living ACC tumor cells at the end of the 72 h incubation period was determined colorimetrically based on the tetrazolium salt MTT as described by Mosmann (1983)). 5-Fluorouracil (5-Fu, as positive control) and the tested sample were compared with a control sample.

2.3. In vivo anti-tumor test

Sarcoma 180 (S-180) tumor cells (1×10^5 cells/mouse) were subcutaneously inoculated into 8-week-old male BALB/c mice weighting 20 ± 1 g. Twenty-four hours later, 5-fluorouracil (5-Fu) and the tested samples were dissolved in 0.9% aqueous NaCl and injected intraperitoneally once a day for 8 days. The same volume of 0.9% aqueous NaCl was injected intraperitoneally into the control mice. The mice were sacrificed on the next day after the last injection, and the tumors were excised. The tumor weights were compared with those in the control mice. The inhibition ratio (ξ) and enhancement ratio of body weight (ϕ) were calculated as follows:

$$\xi = [(W_c - W_t)/W_c] \times 100\% \quad (1)$$

$$\phi = [(W_a - W_b)/W_b] \times 100\% \quad (2)$$

where W_c is the average tumor weight of the control group, W_t is the average tumor weight of the tested group; and W_b and W_a are the body weight of mice before and after the assay. Complete regression is indicated as the ratio of the number of tumor-free mice to the number of mice tested.

2.4. Fluorescence microscopy and apoptotic assessment

ACC tumor cells (1×10^5 cells/mL) from exponential phase cultures were treated with the AAG sample at different time and concentrations, and were incubated simultaneously in RPMI 1640 medium containing 10% fetal bovine serum (FBS) under an atmosphere of 5% CO_2 at 37 °C. Following the treatment, the cells were collected for apoptotic assessment. Apoptosis and necrosis were distinguished by using fluorescence microscopy with Hoechst 33342. Briefly, the cell-permeant dye Hoechst 33342 (10 mg/mL; Sigma) for 15 min in the dark, followed by washing twice with phosphate-buffered saline (PBS), and finally were observed under an inverted phase fluorescence microscope (Olympus DP70, Tokyo, Japan) equipped with a 40× objective and UV filter cube. Cells were shown with blue round nuclei, red round nuclei, blue fragment nuclei and red fragmented nuclei, corresponding to viable, necrotic, apoptotic cells, respectively. Nuclei of apoptotic characteristics including apoptosis were counted and compared numerically to morphologically normal nuclei in the same field. Apoptotic index (AI), which represents the percentage of apoptotic nuclei, was calculated as: AN/TN × 100%, where AN and TN are average number of apoptotic and total nuclei, respectively. Quantitative analysis was performed by counting more than 500 cells in six random fields per sample. Each assay was repeated at least three times.

2.5. Immunohistochemistry for apoptosis-related proteins Bax and Bcl-2

2.5.1. Pretreatment of tumor tissue

S-180 tumors were excised from BALB/c mice and used in the *in vivo* anti-tumor test. The tumors were cut into small pieces, and fixed with formalin for 36 h. Fixed-tumors were dehydrated by immersing in a series from 70%, 80%, 90%, 95% to 100% of graded ethanol solution for 15–20 min. Dehydrated-tumors were passed through successive changes of methyl benzoate until all ethanol was replaced by methyl benzoate. Subsequently, the tumors were embedded in the paraffin. Finally, 4 mm serial sections were cut from the formalin-fixed, paraffin-embedded pretreatment tumor blocks and mounted on poly-L-lysine (PLL)-coated microscope slides, and then were dried at 60 °C for 1 h for immunostaining.

2.5.2. Immunostain of TUNEL

The tumor tissues from treated and control mice were examined by the TUNEL assay to detect the 3′ free hydroxyl ends (3-OH) of the DNA strands created by nucleases in apoptotic cells. Sections of tumor tissues were treated for 20 min with proteinase K (20 μg/mL in PBS), equilibrated for 10 min with TdT buffer, and incubated for 2 h in a TdT mix containing 100 U TdT and 0.5 μL biotin-16-dUTP. Biotin-16-dUTP labeled in 3-OH of DNA was detected by streptavidin-HRP and visualized using DAB for color reaction according to the manufacturer's instructions. Then the sections

were counterstained lightly by methyl green, dehydrated through a graded series of alcohol, cleared in xylene and finally mounted by Permount. The cells whose nucleus turned a distinct brown color were considered as positive cells while the cells whose nucleus turned green were negative cells. The numbers of positive cells were counted with a hemacytometer under a 100× microscope and the mean number was calculated.

2.5.3. Immunostain of Bax and Bcl-2

The tests of Bax and Bcl-2 immunohistochemistry were performed by the peroxidase-labeled streptavidin biotin method with microwave antigen retrieval (Lohmann et al., 2002; Saxena, McMeekin, & Thomson, 2002; Xie, Clausen, Angelis, & Boysen, 1999). Paraffin in the sections were removed by treating with xylene for 15 min twice, and then gradually hydrated through a series from 95%, 80% to 70% of graded ethanol (2 min each) and distilled water (2 min). Endogenous peroxidase was blocked by incubation in 3% hydrogen peroxide (H_2O_2) for 10 min at 37 °C, followed by washing for four times with PBS (5 min each). Antigen retrieval was carried out in a microwave oven. Briefly, the sections were heated to 95 °C in 0.01 M citrate buffer (pH 6.0), and were maintained at this temperature for 10 min, followed by rinsing in warm tap water. And then the sections were treated with normal goat serum for 10 min at 37 °C to reduce nonspecific staining. Subsequently, the rabbit antimouse Bax and Bcl-2 polyclonal antibodies (Santa Cruz Biotechnology Inc., Santa Cruz, CA, US) as primary antibodies were added in optimal dilution and the sections were incubated overnight in a humidified chamber at 4 °C. This step and each of the following were succeeded by washing for four times in PBS for 5 min each. The sections were incubated for 10 min at 37 °C in a humidified chamber with biotinylated goat antirabbit IgG (Zhongshan Golden Bridge Biotechnology Co., Ltd., Beijing, China; 1:200) as secondary antibodies, followed by exposure to streptavidin horseradish-peroxidase (Zhongshan Golden Bridge Biotechnology Co., Ltd., Beijing, China) for 10 min at 37 °C. The color was developed using a solution containing 0.05% diaminobenzidine (DAB) as chromogen and 0.02% H_2O_2. After visualization of horseradish-peroxidase activity by color reaction with DAB, the sections were weakly counterstained with hematoxylin, mounted and examined using light microscope equipped with a 40× objective. To confirm immunospecificity, negative controls consisted of sections in which the primary antibody was omitted and replaced by buffer or a nonimmune IgG. Formalin-fixed, paraffin-embedded sections of normal human lymph node served as positive controls. Both the number of immunoreactive cells and the total number of cells (at least 500 cells) were determined to calculate percentage of Bax and Bcl-2 positive cells by visual inspection of six different fields per section. To assess the apoptosis, ratios of Bcl-2:Bax were determined.

2.6. Statistical analysis

Student's *t*-test was used to evaluate the differences between the controls and tested groups. Significant difference between two groups was defined as $p < 0.05$.

3. Results and discussion

3.1. In vitro and in vivo results

In view of the in vitro inhibition ratio of ACC tumor cells by AAG polysaccharide at different concentrations (0.005 and 0.05 mg/L), the polysaccharide exhibited strong inhibition against cell growth and there was also a dose–response relationship between concentration of AAG and suppression of ACC cell proliferation (Fig. 1). The AAG samples showed inhibition ratios of 23.5% and 34.1% at the concentration of 0.005 and 0.05 mg/L, respectively. It was comparable to 5-Fu (40.4%).

To evaluate the *in vivo* anti-tumor activity of AAG sample, the sample solutions were injected intraperitoneally (i.p. 5, 20 and 40 mg/kg) to BALB/c mice once daily for 8 days after S-180 tumor cells inoculation for 24 h. The results of the *in vivo* anti-tumor activities of the AAG sample are summarized in Table 1, in which also lists that of 5-Fu, a chemotherapeutic anticancer agent as a positive control. The doses of 5, 20 and 40 mg/kg showed inhibition ratios of 16.4%, 39.1% and 37.7%, respectively. The results showed that AAG significantly inhibited tumor growth in dose-dependent way, but all the doses show certain inhibition ratios against tumor-cell growth. The tumor weigh of the control group was 0.81 g, while the tumor weight of mice treated with low, intermediate and high concentration of AAG were reduced to average weighs 0.68, 0.49 and 0.51 g, respectively. The tumor weight of mice treated with a low, intermediate or high dose AAG was significantly lower than that of the control group ($p < 0.05$). Compared with the other dose, the dose 20 mg/kg exhibited highest anti-tumor activities. Moreover, the enhancement ratios of body weight for all the doses weigh significantly higher than that for 5-Fu, indicating that the AAG sample had much lower toxicities than 5-Fu, which kills normal cells as well as cancer cells.

3.2. Fluorescence microscopy and apoptotic assessment

Morphological changes can provide the most reliable criteria for recognizing apoptotic process. Therefore, we utilized fluorescence microscopy to observe apoptosis by changes in cellular morphology, including cell shrinkage, condensation and fragmentation of nuclei, all of which are indicative of apoptosis (Liu, Trimarchi, & Keefe, 1999). Data in Fig. 2 showed nuclear morphology of various type of ACC cell death visualized by fluorescence microscopy with

Table 1
Anti-tumor activity of the AAG sample against Sarcoma 180 solid tumor grown in BALB/c mice.

Sample	Dose (mg/kg × days)	Inhibition ratio (%)	Enhancement ratio weight (%)	Complete regression
Control	20 × 8		28.8	0/10
5-Fu	20 × 8	62.1	18.8	0/10
	5 × 8	16.4*	26.8	0/10
AAG	20 × 8	39.1*	26.9	0/10
	40 × 8	37.7*	26.9	0/10

* $p < 0.05$, significant difference when compared to the control.

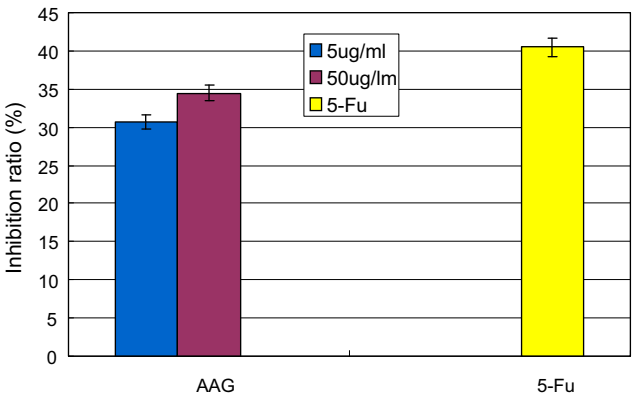

Fig. 1. The in vitro inhibition ratio to the proliferation of ACC by different concentration of the AAG and 5-Fu.

Hoechst staining following exposure to the AAG for 24 h at concentration of 0.5 and 0.05 mg/mL. Hoechst stains the nuclei of cells with a broken or an intact cell membrane. In Fig. 2b and c round nuclei, blue fragment nuclei or shrinkage cells, corresponded to viable and apoptotic cells, respectively. As shown in Fig. 2a, the control group was mainly living cells, while the both concentration had many apoptotic cells with fragmented nuclei. The obvious inhibition against tumor cells indicated that the AAG sample could induce apoptosis in ACC cells.

3.3. Effect of AAG on tumor tissues cell morphology

Fig. 3 shows histological section of tumor tissues in control group and AAG-treated mice. Compared with the tumor tissues of the control group mice, the tumor tissues of AAG sample treated mice showed a massive necrosis such as nucleus atrophy, disintegrating and structure less red staining region. Meanwhile, chromatin condensation, cell shrinkage, plasma membrane blabbing and the formation of membrane-enclosed apoptotic bodies were observed in the tumor sections of AAG-treated mice, indicating many tumor cells were undergoing apoptosis.

3.4. Detection of apoptosis of tumor tissue cells by TUNEL assay

In view of the previous Fluorescence microscopy analysis, we concluded that AAG induced apoptotic cell death in ACC cells. To further confirm the apoptosis of tumor tissues induced by the administration of AAG, the TUNEL assay was performed. As shown in Fig. 4, with an increase of AAG the number of TUNEL-positive cells significantly increased from 5.1% (5 mg/kg) to 9.3% (20 mg/

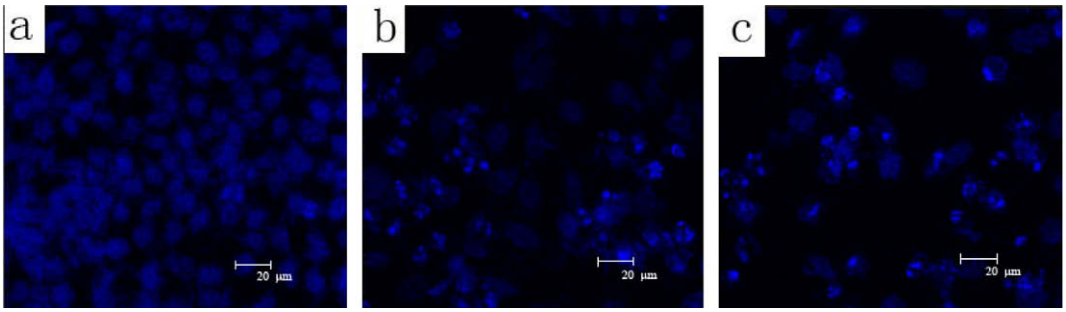

Fig. 2. Nuclear morphology of the various type of cell death was visualized by fluorescence microscopy with Hoechst staining following exposure to the control group (a), AAG-treated concentration of 0.5 mg/mL (b) and 0.05 mg/mL (c).

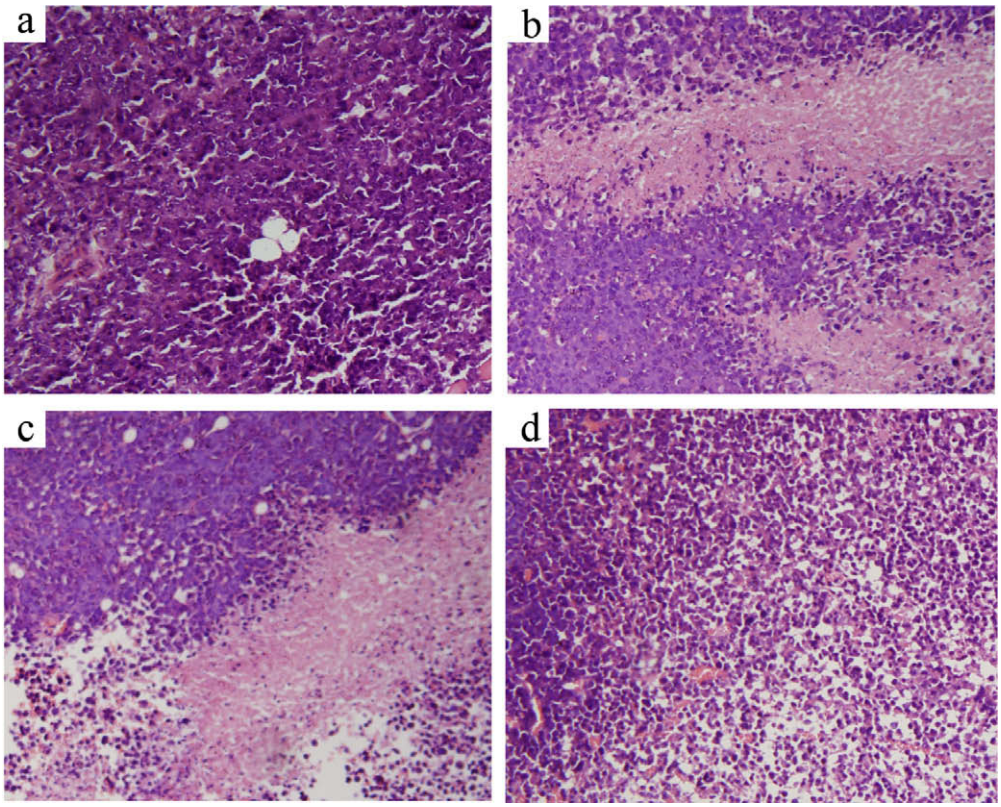

Fig. 3. Histological section of tumor tissues in control group (a), dose 5 mg/kg AAG-treated mice (b), dose 20 mg/kg AAG-treated mice (c) and dose 40 mg/kg AAG-treated mice (d).

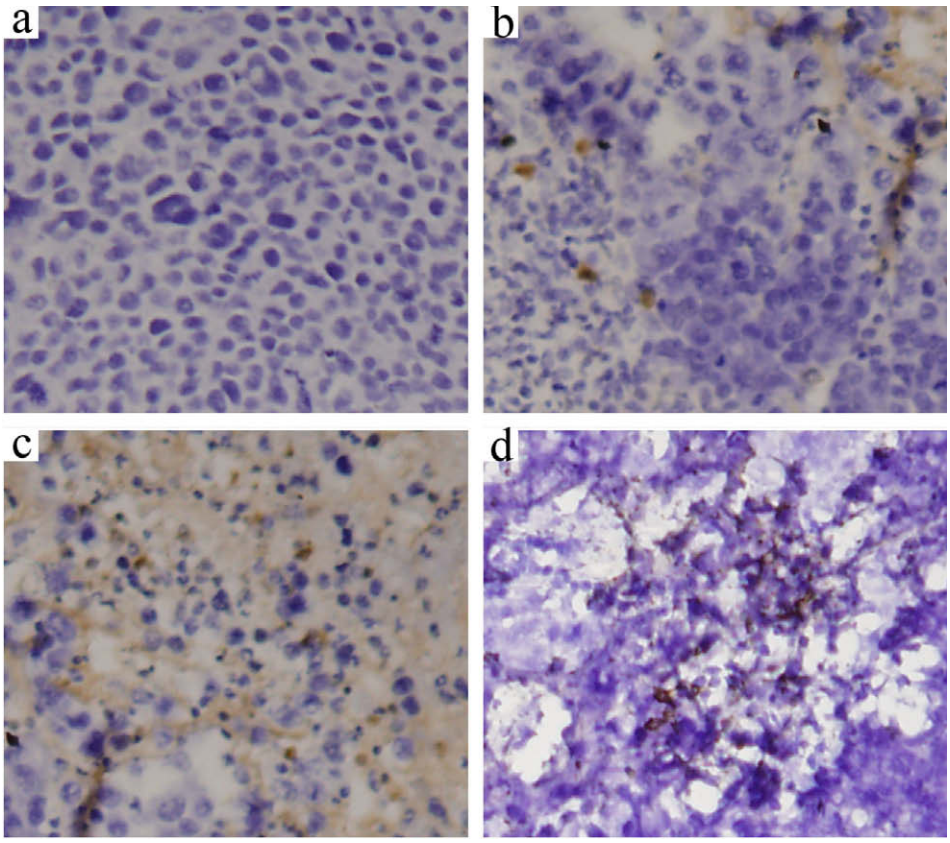

Fig. 4. Apoptotic staining of tumor tissues using a TUNEL technique. Control group (a), dose 5 mg/kg AAG-treated mice (b), dose 20 mg/kg AAG-treated mice (c) and dose 40 mg/kg AAG-treated mice (d).

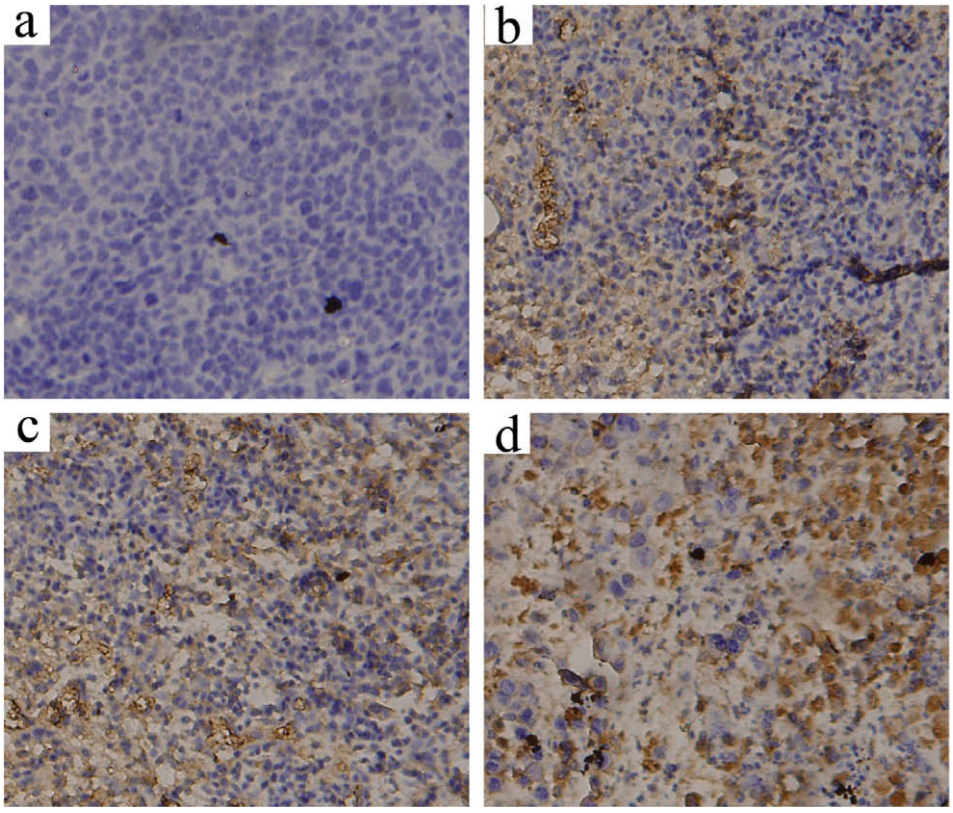

Fig. 5. Bax immunostain in S-180 tumor of the untreated control mice (a), dose 5 mg/kg AAG-treated mice (b), dose 20 mg/kg AAG-treated mice (c) and dose 40 mg/kg AAG-treated mice (d).

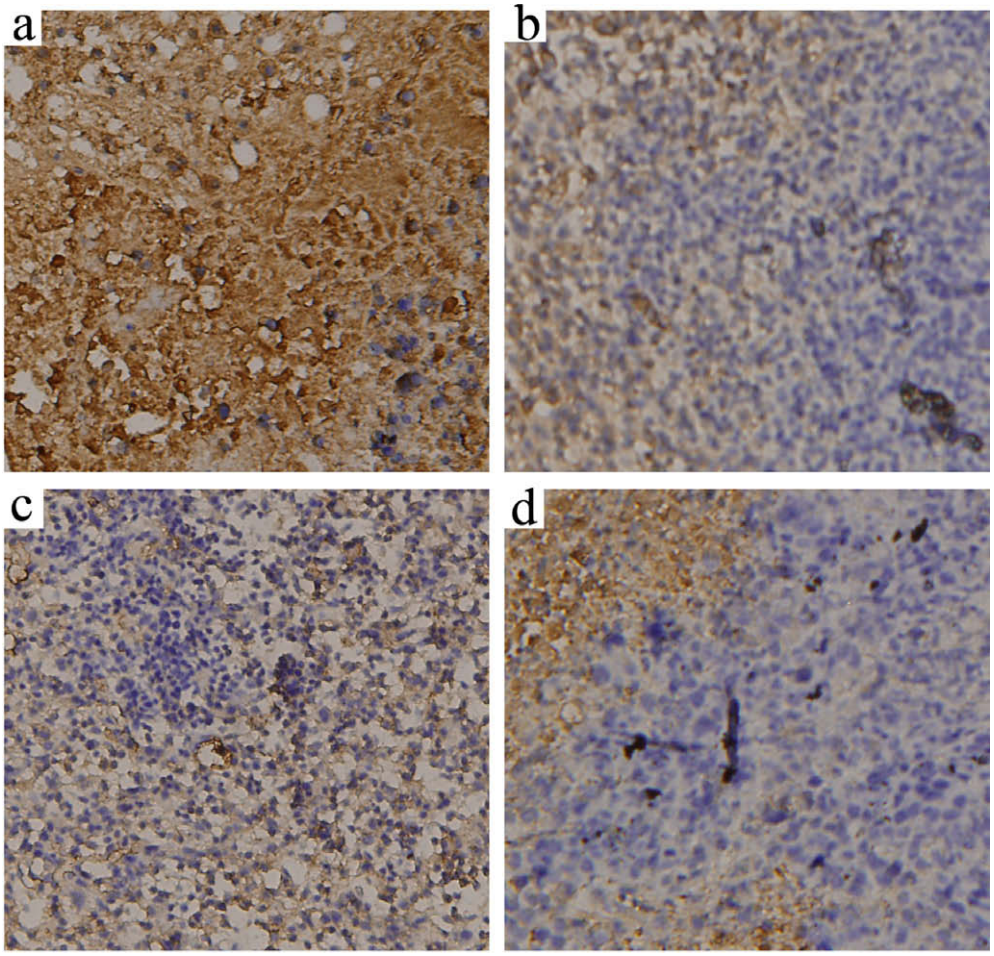

Fig. 6. Bcl-2 immunostain in S-180 tumor of the untreated control mice (a), dose 5 mg/kg AAG-treated mice (b), dose 20 mg/kg AAG-treated mice (c) and dose 40 mg/kg AAG-treated mice (d).

Table 2
The quantitative analysis of the Bax and Bcl-2 immunostaining for S-180 tumor cells in the control and AAG treated groups.

Samples	Bax (% immunoreactivity)	Bcl-2 (% immunoreactivity)
Control group	3.8	58.5
AAG dose 5 mg/kg	30.3*	21.8
AAG dose 20 mg/kg	46.5*	39.6*
AAG dose 40 mg/kg	42.6*	30.7*

* $p < 0.05$, significant difference when compared to the control.

kg) and 7.2% (40 mg/kg), respectively ($p < 0.05$). The apoptotic staining patterns with TUNEL assay corroborated the AAG-induced apoptosis of tumor tissues.

3.5. Immunohistochemistry for apoptosis-related proteins Bax and Bcl-2

Since AAG polysaccharide morphologically induced apoptosis in the tumor cells, the study next investigated if AAG deregulates the apoptotic signal transduction pathway in tumor cells. We have investigated alterations in the expression of apoptosis-related proteins Bcl-2 and Bax in S-180 tumor treated by intraperitoneal injection of AAG aqueous solution into BALB/c mice. Figs. 5 and 6 showed the apoptosis-related proteins Bax and Bcl-2 immunostain in S-180 tumor of the untreated control mice and different dose AAG-treated mice. The results revealed a significant difference in expression of the proteins in control and AAG groups. In the control group, Bax was not detected, whereas Bcl-2 immunostain was significantly strong in S-180 tumor. Compared with the control group, the mice treated with AAG exhibited a significant decreased expression of Bcl-2 and increased expression of Bax. The uniquely high Bax expression with low Bcl-2 immunostain in the AAG group indicated that the AAG polysaccharide induced apoptosis of S-180 tumor cells probably by up-regulating expression of Bax to counteract the effect of Bcl-2. The results from the quantitative analysis of the Bax and Bcl-2 immunostain for S-180 tumor in the control and AAG groups were listed in Table 2. The Bax expression in S-180 tumor after treated with AAG was significantly stronger than that of control group (without exposure to AAG). Simultaneously, after treatment by AAG, expression level of Bcl-2 protein was significantly lower than that of the control group. Furthermore, a high expression level of Bax accompanied by a low Bcl-2 immunoreactivity could sustain a low Bcl-2: Bax ratio in favor of apoptosis, or alternatively, it could effectively antagonize the anti-apoptotic levels of the Bcl-2. The immunohistochemical results indicated that the AAG polysaccharide induced apoptosis in xenograft S-180 tumor cell by up-regulating Bax and down-regulating Bcl-2.

4. Conclusion

AAG polysaccharides isolated from *Auricularia auricula-judae* was water-soluble, and had an M_w of 2.88×10^5. The anti-tumor activities of AAG had been discovered in a dose-dependent manner and the apoptosis in ACC cells could be induced by AAG polysac-

charide. Furthermore, histological examination of the tumor tissue indicated that AAG induced a massive necrosis and infiltration. In addition, apoptosis was also observed from the tumor tissues treated with AAG, which further confirmed by TUNEL assay. Further analysis of the tumor inhibition mechanism revealed that the expression of Bax increased and the expression of Bcl-2 decreased dramatically in S-180 tumor tissue section after injection of AAG. The immunohistochemical results indicated that the AAG polysaccharide could induce apoptosis in S-180 tumor cell by up-regulating Bax and down-regulating Bcl-2. These findings confirmed that the AAG could be considered as a potential anti-tumor agent.

Acknowledgements

This work was supported by a major grant of National Natural Science Foundation of China (30530850) and the High-Technology Research and Development Program of China (2006AA02z102).

References

Baea, J. S., Janga, K. H., & Jinb, H. K. (2006). Effects of natural polysaccharides on the growth and peritoneal carcinomatosis of human gastric adenocarcinoma in a nude mouse model. *Cancer Letters, 235*, 60–68.

Baea, J. S., Janga, K. H., Yimb, H., & Jin, H. K. (2005). Polysaccharides isolated from Phellinus gilvus inhibit melanoma growth in mice. *Cancer Letters, 218*, 43–52.

Baell, J. B., & Huang, D. C. (2002). Prospects for targeting the Bcl-2 family of proteins to develop novel cytotoxic drugs. *Biochemical Pharmacology, 64*, 851–863.

Chen, Y., Cheng, P., Lin, C., Liao, H., Chen, Y., Chen, C., et al. (2008). Polysaccharides from Antrodia camphorata mycelia extracts possess immunomodulatory activity and inhibits infection of Schistosoma mansoni. *International Immunopharmacology, 8*, 458–467.

Gao, Q. P., Seljelid, R., Chen, H., & Jiang, Q. R. (1996). Characterization of acidic heteroglycans from Tremella fuciformis Berk with cytokine stimulating activity. *Carbohydrate Research, 228*, 135–142.

Goodsell, D. S. (2002). The molecular perspective: Bcl-2 and apoptosis. *Stem Cells, 20*, 355–356.

Guo, B., Zhai, D., Cabezas, E., Welsh, K., Nouraini, S., Satterthwait, A. C., et al. (2003). Humanin peptide suppresses apoptosis by interfering with Bax activation. *Nature, 423*, 456–461.

Huang, Q., Zhang, L., Cheung, P. C. K., & Tan, X. (2006). Evaluation of sulfated α-glucans from *Poria cocos* mycelia as potential antitumor agent. *Carbohydrate Polymers, 64*, 337–344.

Khalikovaa, T. A., Zhanaevaa, S. Y., Korolenkoa, T. A. V., Kaledinb, I., & Koganc, G. (2005). Regulation of activity of cathepsins B, L, and D in murine lymphosarcoma model at a combined treatment with cyclophosphamide and yeast polysaccharide. *Cancer Letters, 223*, 77–83.

Lavia, I., Friesemb, D., Gereshc, S., Hadarb, Y., & Schwartza, B. (2006). An aqueous polysaccharide extract from the edible mushroom *Pleurotus ostreatus* induces anti-proliferative and pro-apoptotic effects on HT-29 colon cancer cells. *Cancer Letters, 244*, 61–70.

Lia, G., Kimd, D. H., Kimb, T. D., Parka, B. J., Parka, H. D., Parkb, J. I., et al. (2004). Protein-bound polysaccharide from Phellinus linteus induces G2/M phase arrest and apoptosis in SW480 human colon cancer cells. *Cancer Letters, 216*, 175–181.

Liu, L., Trimarchi, J. R., & Keefe, D. L. (1999). Thiol oxidation-induced embryonic cell death in mice is prevented by the antioxidant dithiothreitol. *Biology of Reproduction, 61*, 1162–1169.

Lohmann, C. M., League, A. A., Clark, W. S., Lawson, D., DeRose, P. B., & Cohen, C. (2002). Bcl-2: Bax and bcl-2: Bcl-x ratios by image cytometric quantitation of immunohistochemical expression in ovarian carcinoma: Correlation with prognosis. *Cytometry, 42*, 61–66.

Ma, Z., Wang, J., & Zhang, L. (2008). Structure and chain conformation of beta-glucan isolated from *Auricularia auricula-judae*. *Biopolymers, 89*, 614–622.

Misaki, A., & Kakuta, M. (1995). Kikurage (tree-ear) and shirokikurage (white jelly-leaf): *Auricularia auricula* and *Tremella fuciformis*. *Food Reviews International, 11*, 211–218.

Misaki, A., Kakuta, M., Sasaki, T., Tanaka, M., & Miyaji, H. (1981). Studies on interrelation of structure and antitumor effects of polysaccharides: Antitumor action of periodate-modified, branched (1 → 3)-beta-D-glucan of *Auricularia auricula-judae*, and other polysaccharides containing (1→3)-glycosidic linkages. *Carbohydrate Research, 92*, 115–129.

Mizuno, T. (1996). Development of antitumor polysaccharides from mushroom fungi. *Thai Food: Finding Ingredients in Japan, 167*, 69–87.

Moradali, M. F., Mostafavi, H., Ghods, S., & Hedjaroude, G. A. (2007). Immunomodulating and anticancer agents in the realm of macromycetes fungi (macrofungi). *International Immunopharmacology, 7*, 701–724.

Mosmann, T. (1983). Rapid colorimetric assay for cellular growth and survival: Application to proliferation and cytotoxicity assays. *Journal of Immunological Methods, 63*, 55–63.

Oltvai, Z. N., Milliman, C. L., & Korsmeyer, S. J. (1993). Bcl-2 heterodimerizes in vivo with a conserved homolog, Bax, that accelerates programmed cell death. *Cell, 74*, 609–619.

Peng, Y., Zhang, L., Zeng, F., & Xu, Y. (2003). Structure and antitumor activity of extracellular polysaccharides from mycelium. *Carbohydrate Polymers, 54*, 297–303.

Ranger, A. M., Malynn, B. A., & Korsmeyer, S. J. (2001). Mouse models of cell death. *Nature Genetics, 28*, 113–118.

Saxena, A., McMeekin, J. D., & Thomson, D. J. (2002). Expression of Bcl-x, Bcl-2, Bax, and Bak in endarterectomy and atherectomy specimens. *The Journal of Pathology, 196*, 335–342.

Schulte-Hermann, R., Grasl-Kraupp, B., & Bursch, W. (1994). Tumor development and apoptosis. *International Archives of Allergy and Immunology, 105*, 363–367.

Tao, Y., Zhang, L., & Cheung, P. C. K. (2006). Physicochemical properties and antitumor activities of water-soluble native and sulfated hyperbranched mushroom polysaccharides. *Carbohydrate Research, 341*, 2261–2269.

Wang, Y., Zhang, L., Li, Y., Hou, X., & Zeng, F. (2004). Correlation of structure to antitumor activities of five derivatives of a β-glucan from *Poria cocos* sclerotium. *Carbohydrate Research, 339*, 2567–2574.

Wolter, K. G., Hsu, Y. T., Smith, C. L., Nechushtan, A., Xi, X. G., & Youle, R. J. (1997). Movement of Bax from the cytosol to mitochondria during apoptosis. *The Journal of Cell Biology, 139*, 1281–1292.

Xie, X., Clausen, O. P. F., Angelis, P. D., & Boysen, M. (1999). The prognostic value of spontaneous apoptosis, Bax, Bcl-2, and p53 in oral squamous cell carcinoma of the tongue. *Cancer Letters, 86*, 913–920.

Zhang, M., Cui, S. W., Cheung, P. C. K., & Wang, Q. (2007). Antitumor polysaccharides from mushrooms: A review on their isolation process, structural characteristics and antitumor activity. *Trends in Food Science & Technology, 18*, 4–19.

Zhang, L., Li, X., Xu, X., & Zeng, F. (2005). Correlation between antitumor activity, molecular weight, and conformation of lentinan. *Carbohydrate Research, 340*, 1515–1521.

Zhivotovsky, B., Orrenius, S., Brustugun, O. T., & Doskeland, S. O. (1998). Injected cytochrome c induces apoptosis. *Nature, 391*, 449–450.